Songklanakarin J. Sci. Technol.
42 (6), 1334-1343, Nov. - Dec. 2020

http://www.sjst.psu.ac.th

Original Article

Stratigraphic and structural evolution of Nakhon Basin, Gulf of Thailand

Nattaphan Bangpa, Christopher K. Morley, Jaydeep Ghosh,
and Niti Mankhemthong*

*Department of Geological Sciences, Faculty of Science,
Chiang Mai University, Mueang, Chiang Mai, 50200 Thailand*

Received: 17 May 2019; Revised: 10 August 2019; Accepted: 18 September 2019

Abstract

The Late Eocene (?)/Oligocene-Recent Nakhon Basin located in the western portion of the Gulf of Thailand has a NW-SE trending half-graben structure controlled by a NE dipping boundary fault on the SW margin of the basin. Six marker horizons were interpreted to determine significant geological events in the basin. Faults are subdivided into two sets based on orientation. The NW-SE, NE dipping boundary fault comprises two segments, Y and X. The two fault segments are inferred to follow NW-SE pre-existing fabrics in the pre-rift section. The N-S trending fault sets are separated into two groups, early syn-rift faults and syn-rift faults. During the syn-rift stage (Oligocene-Middle Miocene), the basin was dominated by N-S early syn-rift faults then segment Y exhibited strong displacement in the Oligocene. The fault grew from several isolated strands, reached a maximum length then towards the end of extension. The western part of the fault remained active while the eastern part was inactive.

Keywords: Nakhon Basin, stratigraphic facies interpretation, modeling of basin evolution, pre-existing fabric, fault development

1. Introduction

The Nakhon Basin is one major rift basins located on the western margin of the Gulf of Thailand (Figure 1a). The basins in the gulf are divided by the N-S trending of the Koh Kra Ridge in two portions which are the eastern portion (large basins e.g. the Pattani Basin) and western portion (small, narrow and elongate basins, e.g. the Nakhon and the Chumphon Basins) (Morley, Charusiri, & Watkinson, 2011; Sautter *et al.*, 2017) (Figure 2a). There is little published information on the study area with regard to seismic stratigraphy, depositional environment and tectonic evolution (Chenrai, 2011). The basin initially formed in the Late Eocene or possibly the Oligocene with deposition continuing to the Holocene (Morley & Racey, 2011). The basin has a half-graben geometry with sedimentary packages expanding toward a boundary fault on the west side (Figure 2b). The orientation of the basin is NW-SE following the east-dipping high angle bounding fault that controls rifting of the basin and provides accommodation space for the syn-rift package. Major and minor unconformities which present in the basin imply changing depositional environments, erosional/non-depositional periods, and variations in sedimentary processes.

This study focuses on understanding how growth faults affected sediment deposition and basin geometry in the context of rift basin evolution. The geometry of the major bounding fault is investigated to understand how the development of the fault controls sediment deposition of the basin. There are significant variations in the footwall geometry of the bounding fault, and the seismic character of sedimentary units on the flexural margin of the half-graben. The boundary fault geometry changes its displacement and orientation in response to subsurface geology. The seismic amplitude, continuity and frequency of sediment packages in the footwall shows differences with the hanging wall sediment packages. Interpretations of 2D and 3D seismic data were used to create a schematic model of the different stages of evolution and environment variation of the Nakhon Basin.

*Corresponding author
Email address: niti.m@cmu.ac.th

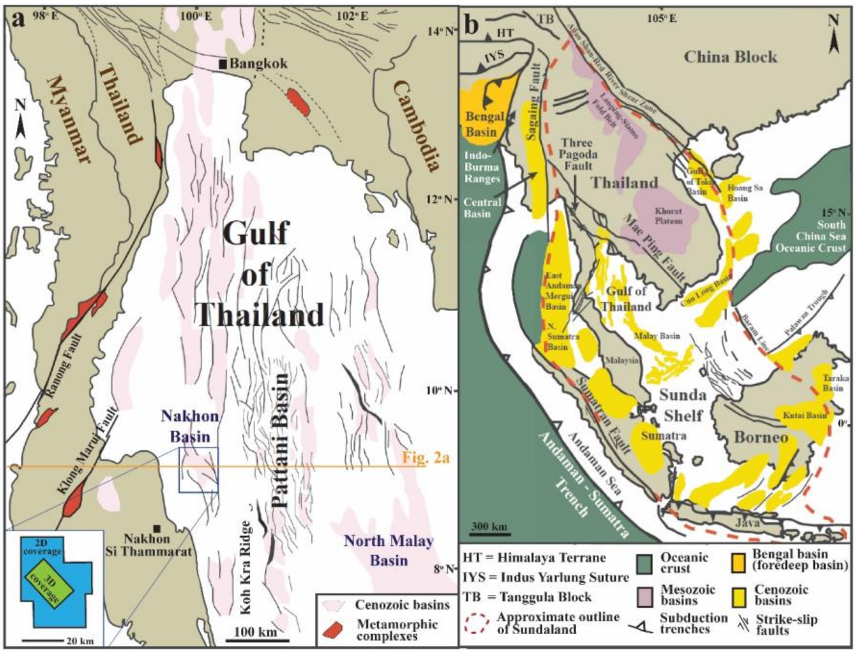

Figure 1. a) Location of the Nakhon Basin in the Gulf of Thailand (a blue rectangle) with an inset figure of area coverage of 2D and 3D seismic data (Coastal Energy, 2012). A solid orange line represents a profile of Figure 2a. b) Regional tectonic map of Southeast Asia region (modified from Searle & Morley, 2011 and Phoosongsee & Morley, 2019).

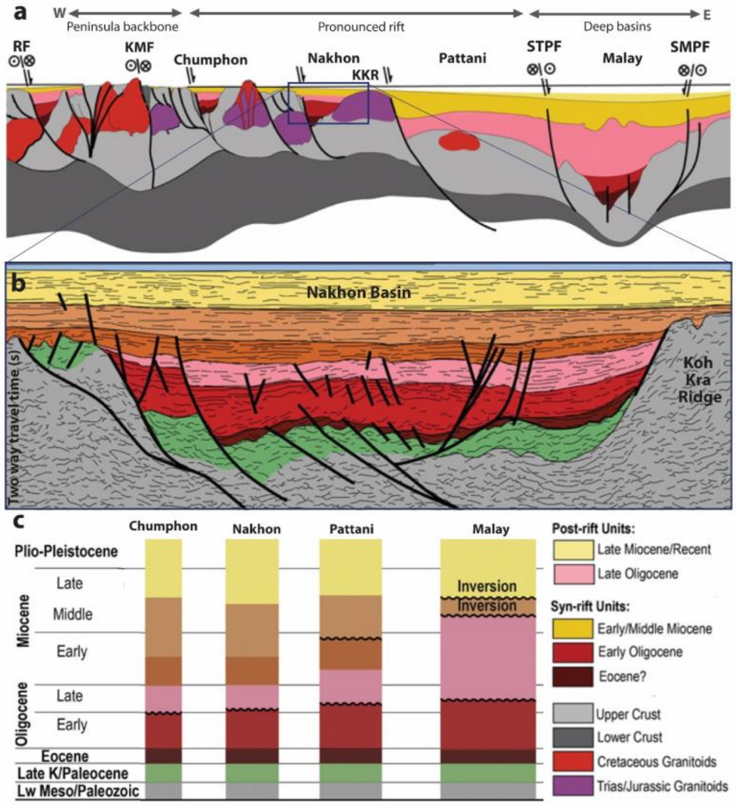

Figure 2. a) W-E cross-section throughout the Cenozoic basins in the Gulf of Thailand (modified from Sautter *et al.*, 2017). RF·is the Ranong Fault; KMF is the Klong Marui Fault; KKR is the Koh Kra Ridge; STPF is the South Three Pagodas Fault; SMPF is the South Mae Ping Fault. b) Stratigraphic interpretation from 2D seismic data of the Nakhon Basin (modified from Sautter *et al.*, 2017). c) Stratigraphic correlation established from seismic data and well data. The stratigraphy of the Chumphon and Nakhon Basins was from unpublished 2D seismic and well data, for the Malay Basin from Mansor, Rahman, Menier, and Pubellier (2014), and for the Pattani Basin from Morley and Racey (2011).

2. Geologic Background

Major tectonic fabric and fault pattern of Cenozoic rifting in Thailand is a result of the India-Eurasian collision in Eocene (Fyhn, Boldreel, & Nielsen, 2010; Tapponnier & Molnar, 1975). It is also partly the result of processes in other parts of the region, for examples, subduction along the Andaman-Sumatra Trench, seafloor spreading in the South China Sea oceanic crust, and the transform boundary along the Ailao Shan-Red River shear zone (Figure 1b) (Pubellier & Morley, 2014; Searle & Morley, 2011). As a consequence of the different geologic setting in each geotectonic terrane, the fault, transfer zone, and fault linkage patterns and the sedimentation sequences can be complex (Morley, 2016).

Extension along predominantly N-S trending fault systems from the northern part of Thailand to the Gulf of Thailand caused formation of Cenozoic rift basins (Morley *et al.*, 2011). The extensional regime contains a large number of Cenozoic basins, which formed between the Paleogene and Middle Miocene (Morley & Racey, 2011). Several models for the origin of the basins have been proposed including their origin as pull-apart basins (Polachan & Sattayarak, 1989), and extensional basins related to the extensional collapse of thickened crust, and subduction rollback in the Andaman Sea (Morley, 2002; Watcharanantakul & Morley, 2000). The basins pass through a region dominated by extension (Gulf of Thailand, Central Thailand), westwards to a region (Shan Plateau) controlled by strike-slip faults that develop pull-apart basins particularly of Late Oligocene-Early Miocene age (Figure 1b) (Morley *et al.*, 2011). Seismic reflection data suggests that the western basins in the Gulf of Thailand are characterized by Late Oligocene-Mid Miocene extension in half-graben basins and Late Miocene-Pliocene post-rift subsidence (Morley & Racey, 2011; Pradidtan & Dook, 1992).

The Nakhon Basin, one of the major Cenozoic extensional basins in the Gulf of Thailand, is a half-graben oriented NW-SE mapped from gravity anomalies and seismic lines (Milsom, 2011). This orientation is oblique to the typical N-S trend of basins in the region. In the Northern part of the basin, extension is accommodated via a large NE dipping low angle normal fault (Chenrai, 2011). A second bounding fault is oriented N-S and dips west, conjugated with an antithetic fault further east. Both faults were active from the Late Eocene (?) to the Middle-Late Miocene (Chenrai, 2011).

The stratigraphy of the Nakhon Basin consists of sediment packages from the Eocene (?) to the Upper Miocene that expand towards the bounding fault zone on the western side of the basin (Figure 2b) (Morley & Racey, 2011). The Eocene syn-rift section was possibly controlled by lower angle normal faults that were later replaced by a higher angle boundary fault. The syn-rift sediments of the basin are restricted to the upper Eocene/Lower Miocene and are sealed by the Middle Miocene post-rift sequences (Figure 2b, c).

3. Materials and Methods

The study area located in the Nakhon Basin covers approximately 1,200 sq km, where 2D or/and 3D seismic reflection surveys are available (Figure 1a). IHS Kingdom software was mainly used for this project. The seismic interpretation, seismic attributes, quantitative interpretation and geological analysis were conducted using this software.

3.1 Seismic interpretation

The faults and key horizons were interpreted based on both 2D and 3D seismic data. The seismic data provide good subsurface images, however the data cannot be shown due to confidentiality as well as information of data depth cannot be given. The seismic data were reinterpreted from Morley (2016). Six horizons were picked in all 2D lines, and every 50 lines for both inlines and crosslines in 3D data. Closer spaced picking (in every 25 lines) was done to achieve more accurate interpretation in areas with complex structure. As the data lacked marker and well information, the key horizons were picked based on seismic characteristics and reflection termination. Faults were picked on all 2D lines and every 25 lines for both inlines and crosslines on 3D data. Fault polygons were generated to determine fault geometry in a map view and to generate time-structure maps.

3.2 Throw - length of fault

Faults tend to express a maximum displacement in the central part of the fault trace that gradually declines toward the tips (Fossen, 2010). The fault displacement history is determined by observing the maximum vertical displacement (throw) of the particular horizons. The throw-length profile along the boundary fault system is composed of linked fault segments and minor splay faults. The throw was calculated by measuring the separation in time of the footwall and the hanging wall for each horizon across the fault plane along the fault strike.

3.3 Isochron map

An isochron map is a contour map representing an equal value of seismic traveltime between selected horizons (Brown, 2010). The map illustrates variations in the stratigraphic thickness of an interval between two horizons or grids. The map illustrates relationships between depositional processes, depocenter location and fault activity.

3.4 Seismic attribute

Seismic attributes are measurements derived from seismic that help to highlight pattern recognition by quantifying the morphological features and amplitude seen in seismic data. A seismic attribute is based on measurements of time, amplitude, frequency, and/or attenuation (Roberts, 2001). Seismic attributes are used to delineate geological features in both structural and stratigraphic images.

3.4.1 Coherence

Coherence is a similarity measurement between traces or waveforms on a processed section. Frequency, amplitude, and phase can change by the acoustic impedance difference and the layer thicknesses below and above the geological boundary (Roberts, 2001). This attribute can identify discontinuities within seismic data from geological elements including stratigraphic features and faults.

3.4.2 Curvature

Curvature is a two-dimensional property of a curve that defines the tightness of a curve at a particular point, or how much the curve deviates from a straight line at a given point (Chopra & Marfurt, 2007). Anticlines exhibit positive curvature, while synclines have negative curvature. Linear (straight-line) parts of a curve have zero curvature. The most-positive curvature identifies the margins of levees and channels, whereas the most-negative curvature emphasizes the thalweg or channel axis (Chopra & Marfurt, 2007).

4. Results and Interpretations

4.1 Horizon interpretations

Six marker horizons (Figure 3) were interpreted in order to understand fault geometry and stratigraphic distribution in the study area. Horizon 1 to Horizon 6 were named as H1 to H6, respectively, in order from the oldest horizon to the youngest horizon. Horizon 1 (H1, green line) marks the top of the basement/base syn-rift section. The top of possible Eocene section was mapped as Horizon 2 (H2, blue line). Horizon 3 (H3, pink line) was interpreted as the top of the Early Oligocene section, Horizon 4 (H4, violet line) as the top of the Late Oligocene section and Horizon 5 (H5, sky blue line) as the top of the Early Miocene section. Horizon 6 (H6, yellow line) is the top of the Middle Miocene post-rift section. This horizon covers all of the study area, even the basement high of upthrow side of the boundary faults.

4.2 Fault interpretations

Faults trend predominantly NW-SE and N-S. One of them is the NE dipping, NW-SE trending boundary fault (NBF; Figure 4b). The N-S direction is followed by major and minor faults (Figure 4a). The NE dipping boundary fault bifurcates into Segments X and Y. Both segments dip steeply (60°-70°) in the shallow sections and gently (35°-45°) in the deep sections. Segment X turns to a N-S trend and terminates in the center of the fault. Segment Y is the main fault that controls the basin along with the NW-SE trend. Segment Y exhibits high displacement especially in the syn-rift sections and loses displacement passing up section (e.g. Horizons 3 and 4) and dies out before the upper syn-rift sections (Figures 3 and 5a). Segment X shows lower displacement than the segment Y and also exhibits decreasing fault displacement in the shallow section. Segment X cuts Horizons 4, 5, and 6 (Figure 3). These relationships indicate that Segment Y has developed before Segment X.

The other trend of faults in the study area is N-S. The faults can be subdivided into two groups, early syn-rift faults and main syn-rift faults. The early syn-rift faults (Faults P and Q; Figure 5b) lie in the center of the study area. These faults are characterized by high displacement that can be observed in the base-syn rift level (Horizon 1). The displacement gradually decreases in the upper section. Some of these faults terminate in the early syn-rift section. However, some faults extend to the upper section (late syn-rift and transition) or are linked to the syn-rift faults (Figure 5b).

The syn-rift faults are the other group of N-S trending faults. These faults are located in the middle of the study area and have a fault length of approximately 2.8 km. The faults dip toward the east and west and exhibit an en-echelon rotated fault block style (Figure 5c). Some of these are recognized as listric faults with dips in the shallow part around 65°-70° and lower dipping angle (35°- 45°) in the deep part. The fault group probably nucleated within the syn-rift section and propagated radially. The faults die out in the syn-rift-post-rift transitional section. Some faults extend to post-rift section (Figure 5c).

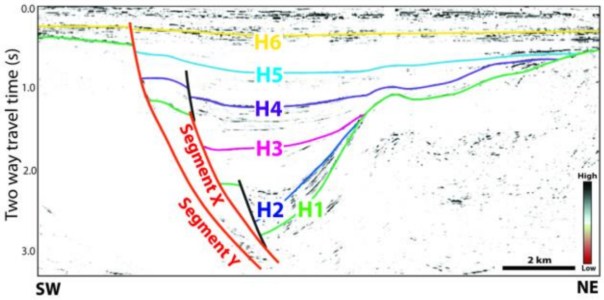

Figure 3. Dim 2D vertical seismic section across the basin shows six interpreted horizons and the basin boundary faults (Segments X and Y). See Figures 4 and 5 for the location.

4. 3 Fault activity (Throw-length profile)

A throw-length profile plot was created along the strike of the boundary fault to investigate activities of the boundary fault (NBF, Figures 3 and 6). The throws of Segments X and Y were summed to provide the total throw of the boundary fault (Figure 6). In general, throw of the boundary fault decreases up section. Due to the lack of seismic data in the NW, we cannot observe the NW fault tip, and the fault shows high throw at the first point of measurement (Location 1, Figure 6). The throw of Horizons 1 and 2 is high in the NW, and then it decreases in the middle part of the fault and shows minimum displacement at Location 5. After that, the throw gradually increases toward the SW and then rapidly decreases at Location 6 and terminates at Location 7. Horizon 3 does not show boundary fault throw in the middle part and NW part, because of the horizon onlaps to the inactive basement high in those areas.

The throw distribution patterns of Horizons 4, 5, and 6 are comparable. The throws of these three horizons are measured only in Segment X as the Segment Y ceased. At Location 4 (Figure 6), the throw dramatically decreases as the throw measurement of Segment X is stopped at Location 3. At Locations 2, 5, and 6, the displacement abruptly decreases due to a presence of splay faults or hard-linkage as strain transfers to these faults especially for Horizons 1, 2, and 3.

5. Discussions

5.1 Orientation and development of the boundary fault

The NE dipping boundary fault of the Nakhon Basin strikes NW-SE and its development control the basin geometry. The boundary fault orientation is different from adjacent basins in the western portion of the Gulf of Thailand

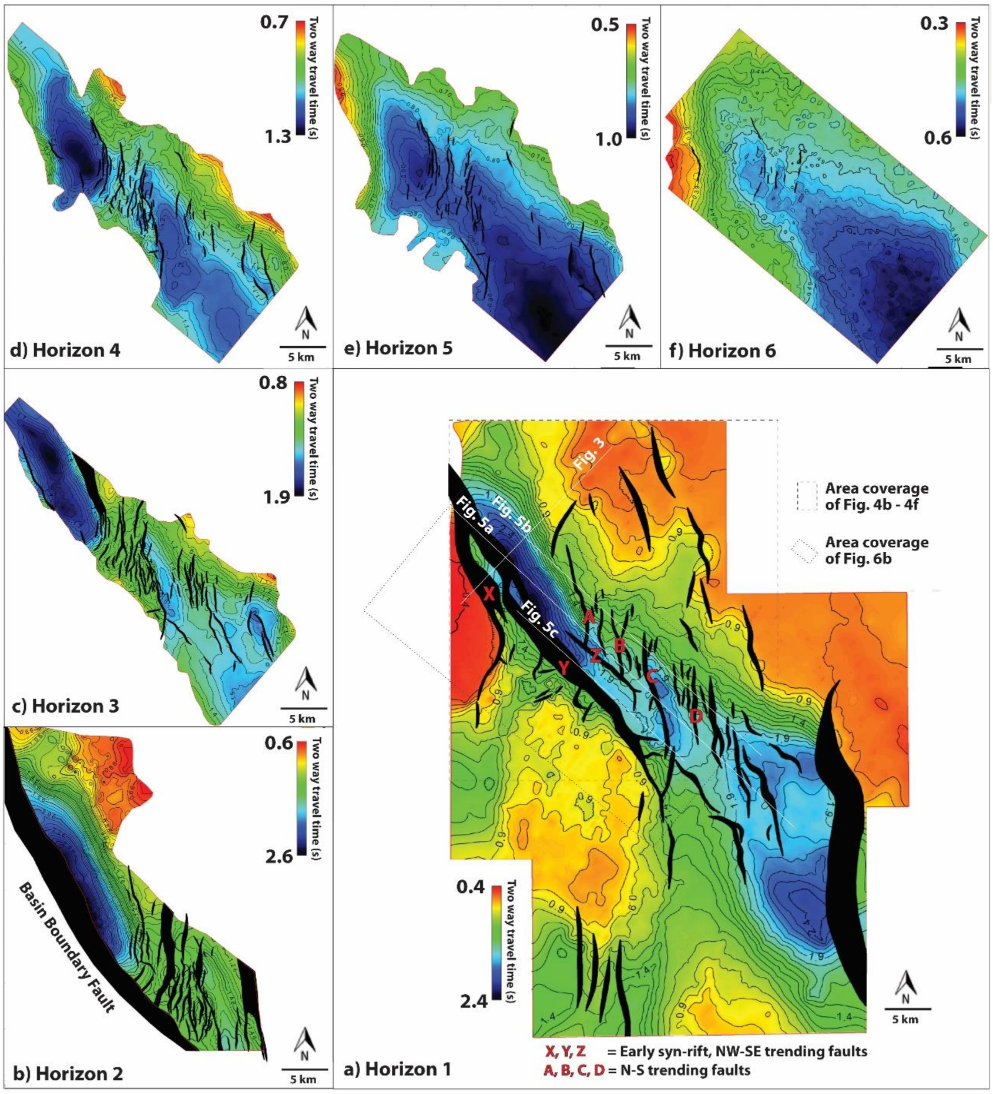

Figure 4. Time structural map of Horizons 1-6 (H1-H6) showing the boundary fault (NBF) consists of two segments, Segment X and Segment Y. The early syn-rift faults trending N-S are marked as Segments A, B, C, and D.

(the Chumphon and Songkhla Basins). The boundary fault shows a high amplitude zone and significant displacement in the pre-rift section. Fault Z (Figure 7a, 7b) strikes NW-SE and is the most unambiguous indication of a basement trend, which suggests that the boundary fault followed a similar trend.

The Nakhon Basin boundary fault is subdivided into Segments X and Y. Segment Y possibly consists of initially multiple individual faults and that have linked together. In the pre-rift stage, there are four individual faults: M, N, O, and Z (Figure 7a). These segments strike NW-SE. In the early syn-rift stage, the segments M, N, and O linked together and developed into a single large fault, i.e., Segment Y (Figure 7b). During the middle to late syn-rift stages, Segment Y was strongly active and associated with high displacement and then became inactive as it died out in the Late Oligocene section (Figure 7c, 7d). Segment X initiated and linked with Segment Y and became fully developed and had high displacement (Figure 7c, 7d).

In the syn-post rift transition stage, Segment X decreased displacement in the upper part of the section. The southern tip of this segment turns to a N-S direction as a result of the fault diverging from the pre-existing trend to follow the regional extension direction (Figure 7e). The extension direction was predominantly E-W. The boundary fault strikes the NW-SE direction, and the presence of the second trend of faults trending N-S indicates that early on in the history of the rift the boundary fault developed along a discrete NW-SE trending zone of weakness in the basement, oblique to the W-E extension direction. The influence of this zone of weakness was strong during pre and early syn-rift stages but declined during the late syn and post-rift stages.

5.2 Basin evolution and modeling

The Nakhon Basin initiated rifting along with early N-S and NW-SE trending fault sets in the late Eocene (?) or

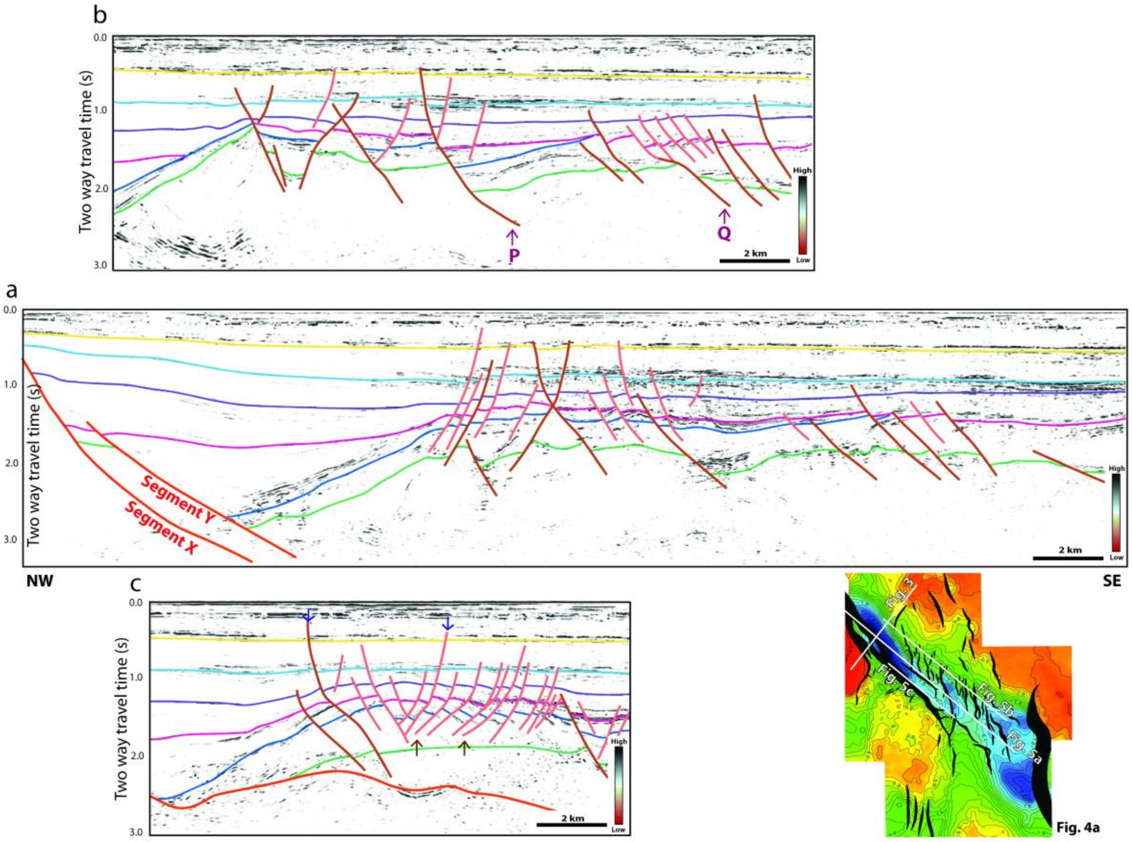

Figure 5. Dim 2D vertical seismic sections of fault interpretations. a) Regional seismic section across the study area shows the interpretation of horizons and faults. b) The example of early syn-rift faults (Faults P and Q) shows high displacement on Horizon 1 and links to the syn-rift faults in the upper sections. c) Main syn-rift faults represent west and east dipping, en-echelon normal fault style. Brown arrows point out listric faults, and blue arrows are the examples of faults that propagate to the post-rift transition (Horizon 6).

Early Oligocene (Figure 8a) based on analogy with the nearby Songkhla Basin (Morley & Racey, 2011). The basin is controlled by the N-S early syn-rift faults showing strong displacement on the base syn-rift Horizon (H1). The depocenter is located adjacent to the early syn-rift faults indicating their influence on the basin rather than the boundary fault. The western boundary fault developed (Segment Y; Figure 8b) with high displacement during the Early Oligocene; Segment X formed during this time resulting in the basin exhibiting the half-graben basin geometry. The sediment package strongly exhibits expansion toward the boundary fault (Segment Y).

Segment Y died out during the Late Oligocene (Figure 8c), while Segment X became more strongly active and shows high displacement. The entire N-S en-echelon syn-rift faults are active into the upper sections. The basin developed until the Early Miocene. The Miocene depocentre is located in the center of the basins where the topography is low (Figure 8d).

The syn-rift-post-rift transition stage occurred during the Middle Miocene (Figure 8e). Some syn-rift faults extend into this section and exhibit sufficient displacement that affects the geometry of the sediment package expanding toward the syn-rift fault. Faulting ceased since Late Miocene (Figure 8f). From the Late Miocene onwards, the basin was stable without major tectonic activity, and sedimentation was independent of any boundary fault control.

5.3 Basin environment variation

The depositional environments of the basin change through time in responding to basin evolution particularly the boundary fault development (Phoosongsee & Morley, 2019). In the first stage (Figure 9a), the basin was possibly dominated by fluvial systems. Small alluvial fans formed along the boundary fault-bounded uplifted footwall. In the second stage (Figure 9b), the boundary fault predominately influenced the basin, with the sediment package shows thickening toward the boundary fault. Alluvial fans are well developed along the fault scarp. In fluvial systems, alternating packages of sand and shale are dominant away from the boundary fault zone, which may comprise alluvial fans (Morley & Racey, 2011). During the third stage (Figure 9c), Segment X of the boundary fault was strongly active and Segment Y became inactive. Small channels and moderate amplitude continuous reflectors from the floodplain/lacustrine shales are observed. The interpretation implies that a low energy fluvial environment was dominant in the basin. During the fourth stage (Figure 8d), high energy fluvial systems probably dominated the basin as broad channels are identified in the upper section. After that, the basin environments are assumed to have fluctuated between marine and continental condition since this is the general pattern for the Gulf of Thailand (Morley & Racey, 2011).

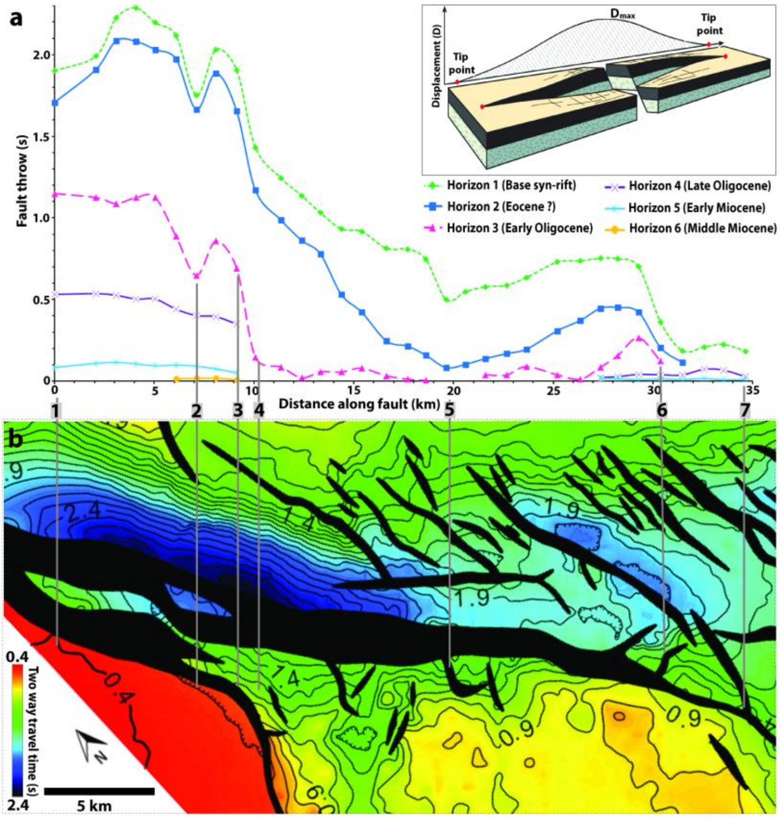

Figure 6. a) Fault throw profile along the boundary fault. b) Time structural map of the top of basement/base syn-rift. Coverage of cropped structural map is shown in Figure 4a. Inset figures display a displacement profile indicating maximum displacement near the center (modified from Fossen, 2010).

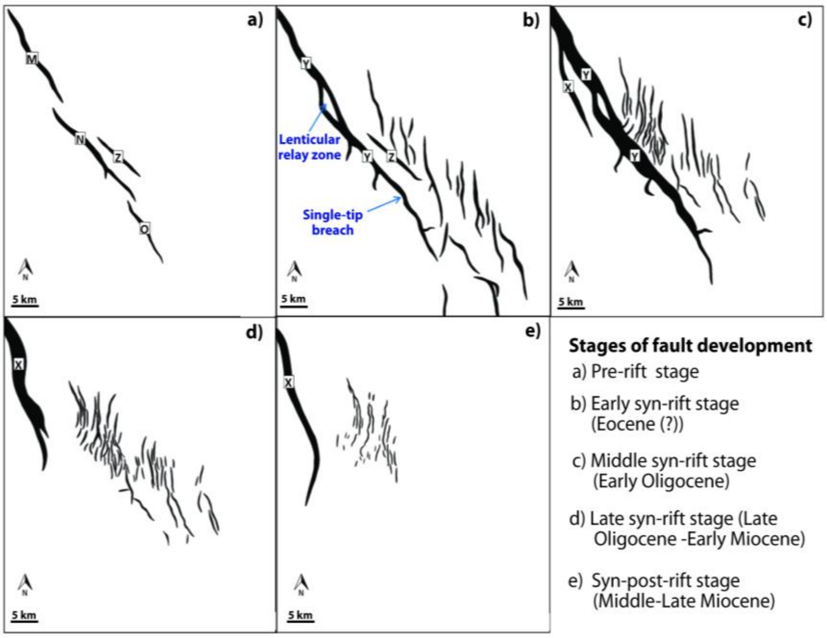

Figure 7. Fault development through time. a) Pre-rift stage, b) Early syn-rift stage (Eocene (?)), c) Middle syn-rift stage (Early Oligocene), d) Late syn-rift stage (Late Oligocene-Early Miocene), and e) Syn-post-rift stage (Middle-Late Miocene).

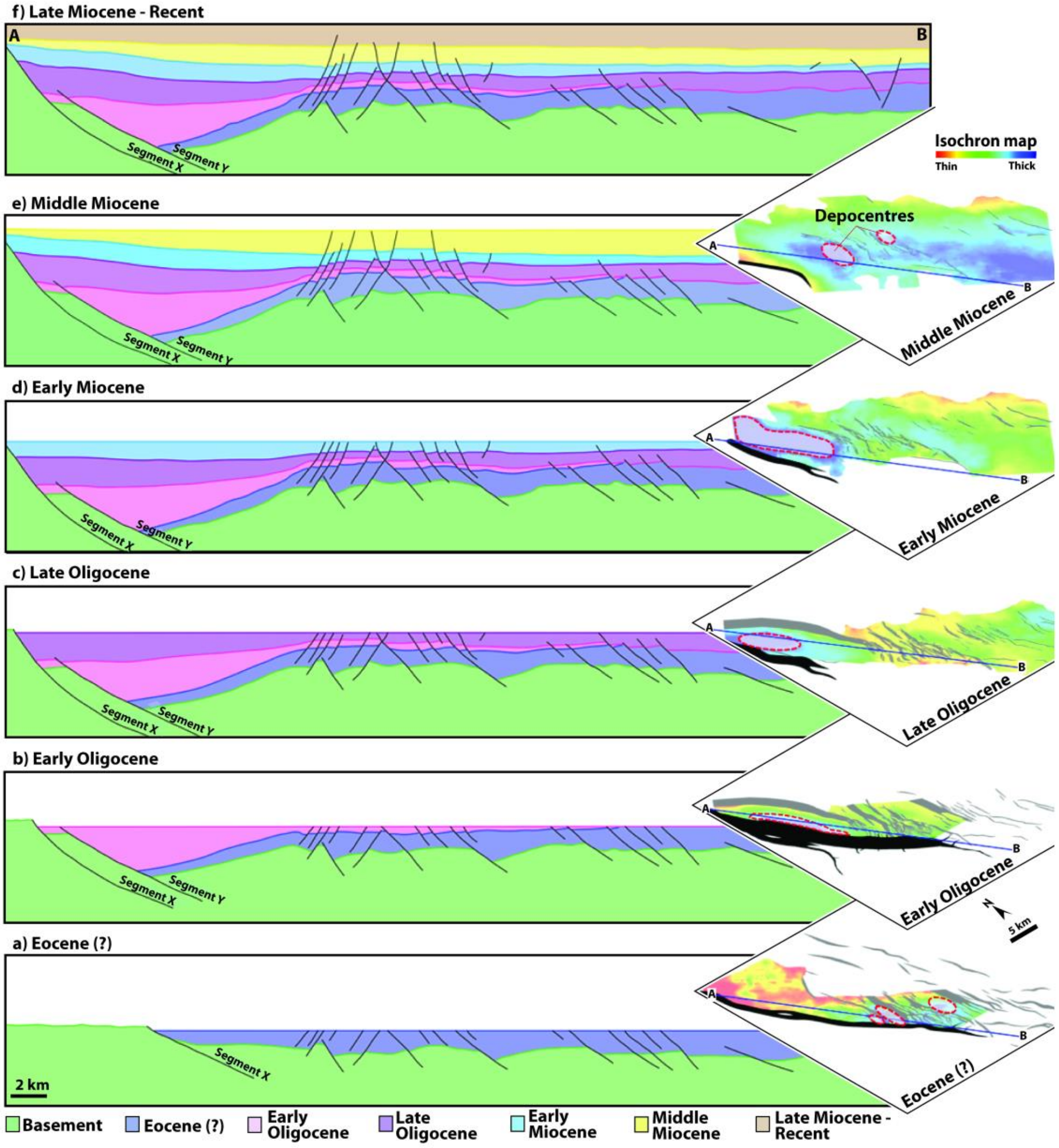

Figure 8. Schematic models of the Nakhon Basin evolution with isochron maps in a) Eocene (?), b) Early Oligocene, c) Late Oligocene, d) Early Miocene, e) Middle Miocene, and f) Late Miocene-Recent. Isochron maps show depocenter locations (dashed red polygons) for each stage of development.

6. Conclusions

The Nakhon Basin is an Eocene (?) to Middle Miocene half-graben, where the boundary fault orientation is affected by pre-existing fabrics. The boundary fault is located on the SW side of the basin and trends NW-SE and dips toward NE. The fault can be subdivided into two branches including Segments X and Y. Both segments follow a discrete zone of weakness zone in the pre-rift section. Segment Y controls the basin formed by the linkage of the three individual fault segments in the early stage of rifting. The N-S faults are separated into two sets, early syn-rift and syn-rift faults. Two other fault sets were identified, both trend N-S, but differ regarding timing. Hence they are separated into early syn-rift and syn-rift faults. The early syn-rift faults are characterized by high displacement at the base syn-rift horizon and die out or link with the syn-rift faults in the upper sections. The N-S early syn-rift faults are dominant in the youngest syn-rift section where the influence of the pre-existing fabric declines. The syn-rift faults are conjugate normal faults with en-echelon map patterns. These faults are dominant in the basin during the syn-rift-post-rift transition stage.

The environment of the basin in the early stage is probably a fluvial system since narrow channels, and moderate amplitude continuous reflectors from floodplain/ lacustrine shale are identified. Alluvial fan and coarse clastic sediments deposition adjacent to the boundary fault is charac-

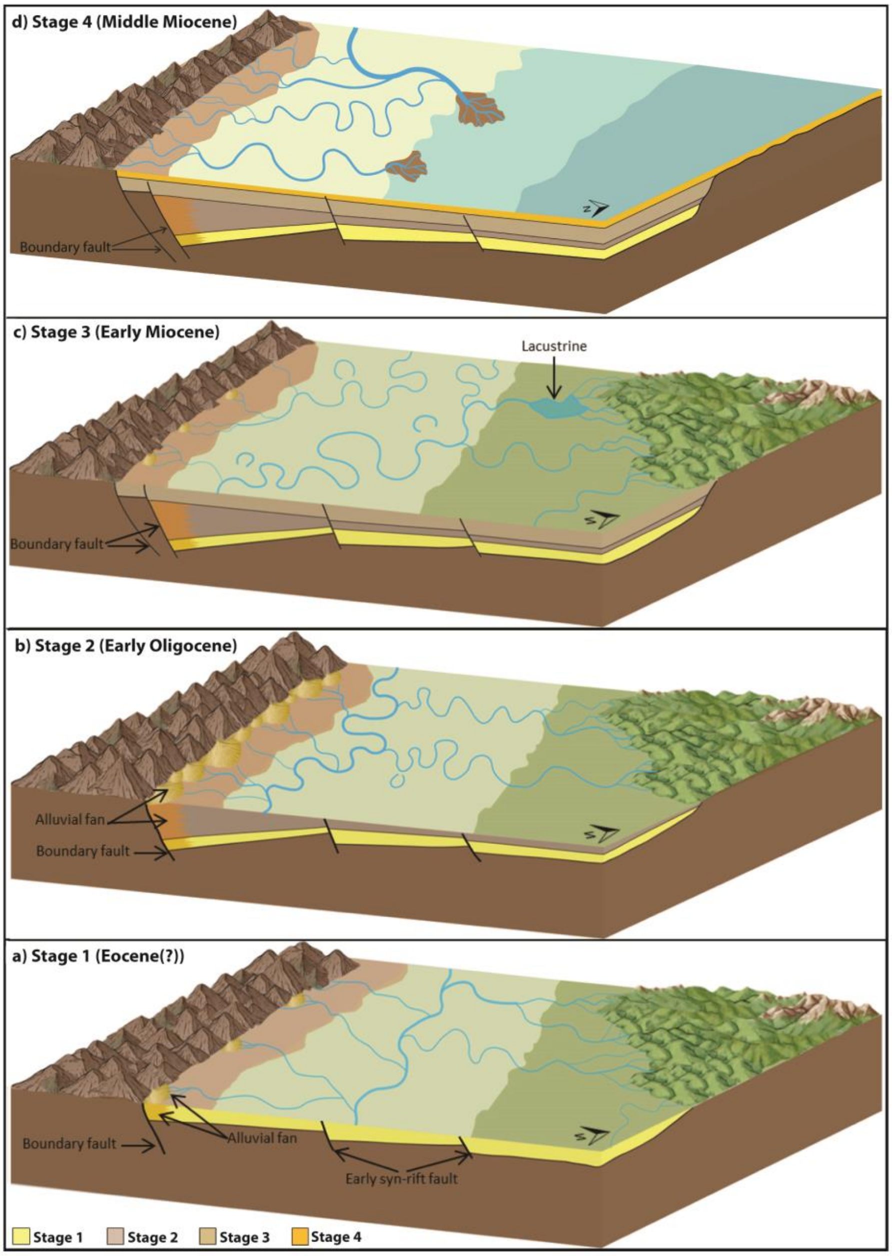

Figure 9. Basin environment variations through time. a) Stage 1 (Eocene(?)), b) Stage 2 (Early Oligocene), c) Stage 3 (Early Miocene), and d) Stage 4 (Middle Miocene).

terized by moderate amplitude, chaotic reflectors. Marine condition influences the basin when the basin is gradually subsiding in the post-rift stage, and was probably episodically present during the syn-rift stage too.

Acknowledgements

We are grateful to Petroleum Geophysics Program, Department of Geological Sciences, Chiang Mai University for the IHS Kingdom software supports and PTT Exploration and Production Public Company Limited for a research scholarship. We thank anonymous reviewers for comments that improved the manuscript. The seismic data were reinterpreted from Morley (2016). This work was selected for publication from the 8th International Conference on Applied Geophysics, Songkhla, November 8-10, 2018.

References

Brown, A. R. (2010). Interpretation of three dimensional seismic data. *AAPG Memoir 42, SEG Investigation in Geophysics, No. 9* (7th ed.). Tulsa, Ok: AAPG and SEG.

Chenrai, P. (2011). Structural style and tectonic evolution of the Nakhon Basin, Gulf of Thailand. *Bulletin of Earth Sciences of Thailand, 4*, 70-75.

Chopra, S., & Marfurt, K. (2007). Seismic curvature attributes for mapping faults/fractures, and other stratigraphic features. *Recorder, 32*, 37-41.

Coastal Energy. (2012, March 31). Offshore Thailand. Retrieved from http://www.coastalenergy.com/operations/offshore- thailand.html

Fossen, H. (2010). *Structural geology*. Cambridge, England: University Printing House.

Fyhn, M., Boldreel, L., & Nielsen, L. (2010). Escape tectonism in the Gulf of Thailand: Paleogene left-lateral pull-apart rifting in the Vietnamese part of the Malay Basin. *Tectonophysics, 484*, 365-376. doi: 10.1016/j.tecto.2009.11.004.

Mansor, M. Y., Rahman, A. H., Menier, D., & Pubellier, M. (2014). Structural evolution of Malay Basin, its link to Sunda block tectonics. *Marine and Petroleum Geology, 58*, 736-748.

Milsom, J. (2011). Regional geophysics. In M. F. Ridd, A. J. Barber, & M. J. Crow (Eds.), *The geology of Thailand* (pp. 493-506). London, England: Geological Society.

Morley, C. K. (2002). A tectonic model for the Tertiary evolution of strike-slip faults and rift Basins in SE Asia. *Tectonophysics, 347*, 189-215. doi:10.1016/ S0040-1951(02)00061-6.

Morley, C. K. (2016). The impact of multiple extension events, stress rotation and inherited fabrics on normal fault geometries and evolution in the Cenozoic rift basins of Thailand. In C. Childs, R. E. Holdsworth, C. A.-L. Jackson, T. Manzocchi, J. J. Walsh, & G. Yielding (Eds.), *The geometry and growth of normal faults* (Vol. 439, pp. 413-445). London, England: Geological Society.

Morley, C. K., & Racey, A. (2011). *Tertiary stratigraphy, The Geology of Thailand* (Vol. 10, pp. 223-271). London, England: Geological Society.

Morley, C. K., Charusiri, P., & Watkinson, I. M. (2011). *Structural geology of Thailand during Cenozoic, The Geology of Thailand* (Vol. 11, pp. 273-334). London, England: Geological Society.

Phoosongsee, J., & Morley, C. K. (2019). Evolution of a major extensional boundary fault system during multi-phase rifting in the Songkhla Basin, Gulf of Thailand. *Journal of Asian Earth Sciences, 172*, 1-13.

Polachan, S., & Sattayarak, N. (1989). Strike-slip tectonics and the development of tertiary basins in Thailand. *International Symposium on Intermontaine Basins: Geology and Resources* (pp. 243-253). Chiang Mai, Thailand: Chiang Mai University.

Pradidtan, S., & Dook, R. (1992). Petroleum geology of the Northern part of the Gulf of Thailand. *National Conference on Geologic Resources of Thailand: Potential for Future Development* (pp. 235-246). Bangkok, Thailand: Department of Mineral Resources.

Pubellier, M., & Morley, C. K. (2014). The basins of Sundaland (SE Asia): Evolution and boundary conditions. *Marine and Petroleum Geology, 58*, 555-578.

Roberts, A. (2001). Curvature attributes and their application to 3D interpreted horizons. *First Break, 19*, 85-99.

Sautter, B., Pubellier, M., Jousselin, P., Dattilo, P., Kerdraon, Y., Choong, C. M., & Menier, D. (2017). Late Paleogene rifting along the Malay Peninsula thickened crust. *Tectonophysics, 710-711*, 205-224.

Searle, M. P., & Morley, C. K. (2011). Tectonic and thermal evolution of Thailand in the regional context of SE Asia. In M. F. Ridd, A. J. Barber, & M. J. Crow (Eds.), *The Geology of Thailand* (pp. 539-571). London, England: Geological Society.

Tapponnier, P., & Moinar, P. (1975). Cenozoic tectonics of Asia: Effects of a Continental Collision. *Science, 189*, 419-426.

Watcharanantakul, R., & Morley, C. K. (2000). Syn-rift and post-rift modeling of the Pattani Basin, Thailand: Evidence for a ramp-flat detachment. *Marine and Petroleum Geology, 17*, 937-958.